# EXTENDING FOULING CONCEPTS FROM HEAT EXCHANGERS TO PROCESS EQUIPMENT

**A.P. Watkinson[1], Z. Fan[2] and B. Petkovic[1]**

[1] Dept. Chemical & Biological Engineering, University of British Columbia, Vancouver, BC Canada V6T 1Z3
[2] Canmet ENERGY, Natural Resources Canada, Devon, Alberta Canada T9G 1A8
apw@chbe.ubc.ca

## ABSTRACT

In petroleum processing, fouling occurs in equipment such as conversion, treating and separation units as well as in heat exchangers and fired furnaces. Challenges in translating lab deposition data to plant units include not only the usual scale-up issues, but problems in understanding both the phase behaviour in systems with many heavy components, and the process by which deposits are formed from the heavy hydrocarbon species. This requires additional modeling steps to interpret fouling results. Examples are presented of two such problems in fluid coking units: cyclone exit line fouling, which is thought to be a vapour phase problem, and scrubber grid fouling which is due to deposition of heavy oil aerosol droplets. In each case, lab results are presented, lab and plant conditions are compared, and model calculations are used to understand fouling under industrial conditions.

## INTRODUCTION

Fouling in process plants is not limited to shell and tube exchangers. In processing heavy oils, in particular, deposition can occur throughout the plant. Applying deposition results from lab-scale facilities to large-scale process units raises different challenges from those normally addressed when dealing with shell and tube heat exchangers. In the laboratory, with a single tube unit test rig, one can readily approach the Reynolds number or wall shear stress for the shell and tube heat exchanger. However it is more difficult to match the high Reynolds numbers or wall shear stresses in other process units, particularly in vapour phase flows. Although elements of mechanisms may be the same (eg transport, adhesion, ageing), scale-up issues can be very different than is the case for projecting single-tube lab results to shell and tube heat exchangers. Two cases are discussed which illustrate challenges to solving industrial equipment fouling problems via typical laboratory fouling studies.

Coking units are commonly used in upgrading of heavy oils (Wiehe, 2008). Within fluid cokers (Figure 1; Hammond, 1998), coking on vessel walls is a serious problem, but the cyclone unit through which the product vapours pass, also can cause shut-downs due to pressure build-up and blockage. Coke is injected into the vapour upstream of the cyclone to aid in scouring, such that fouling is limited within the body of the cyclone. Droplets larger than about 8 microns in diameter should be captured in the cyclone, and not enter the exit line. However build-up can become serious in the relatively large diameter (>0.5-m) but short exit line of the cyclone. The flow is highly turbulent, and the fluid may undergo slight cooling. Some carryover of fine coke particles from the fluid bed may occur, although examination of deposits suggests that this is not a major mechanism of fouling. Once formed, deposits age rapidly because of the high temperatures (500°C). There may be several cyclones in parallel within the coker vessel, so flow distribution can affect deposition in a given cyclone. In the countercurrent scrubber mounted above the coker, vapours leaving the cyclone are cooled and heaviest components are to be removed from the vapours. Cooler wash liquids enter at the top of the scrubber, are sprayed down over a scrubber grid of structured packing, and then enter a zone of sheds whose role is to provide some contact, and re-distribute the liquid wash oil, which eventually falls into the scrubber pool for recycling to the coker feed. Although deposits accumulate in the sheds of the scrubber, a more critical problem has been the build-up in the scrubber grid packing. This paper describes experimental approaches and challenges which face efforts to understand fouling in these two situations.
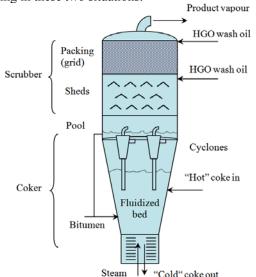


Figure 1 Schematic representation of a Fluid Coker.

## CYCLONE EXIT LINE FOULING

Examination of aged plant deposits suggests that the origin of the deposition problem is not in coke particles carried over from the fluid bed, but rather is associated with the vapours which can contain high molecular mass species. Alternative hypotheses state that the origin of coke-like deposits was either vapour phase coking reactions, or physical condensation of heavy liquid species. This situation was studied experimentally and by simple modeling."

## Laboratory Study

Figure 2 is a flowsheet of a bench-scale coking unit (Zhang and Watkinson, 2005) used for the experiments. The coker is an externally heated 7.5 cm dia. × 1 m tube equipped with an atomization system, and a 15 cm dia. freeboard section with internal filters to remove coke particles and large droplets, such that fouling would arise only from the product vapour. Test sections for mass deposition measurements include an external cyclone with a short exit tube, and an additional 90-cm. long Type 304 stainless steel vertical tube, for which results are presented. Bitumen which contained 55% vol. material boiling at over 524°C, was fed at 0.3 kg/h, typically along with 0.3 kg/h steam and 0.2 kg/h nitrogen. Fouling rates in runs lasting 6-h were calculated from the test section weight increase and are expressed as deposit yield, the mass of deposit/mass of bitumen fed. Filtration tests showed no coke particles passed through into the test section, and suggested that for the 10-micron filter, vapours or a fine aerosol mist only contribute to the deposit build-up.
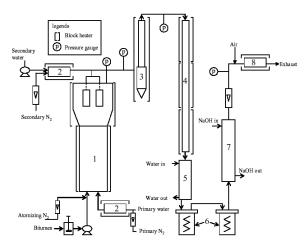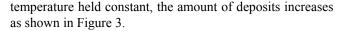


Figure 2 UBC Cyclone Fouling Test Rig
Legend: 1-Coking reactor with filters in freeboard; 2-Sec. Steam Generator; 3-Cyclone + Short Exit Tube; 4-Long Tube Section; 5-Condenser; 6-Liquid Product Accumulators; 7-Scrubber; 8-After-burner.

Experiments were done varying both the reactor (coker) temperature $T_R$, at which the vapours are produced, and the downstream test section temperature $T_D$, at which the deposits form. When $T_R$ is fixed, vapour quality and quantity 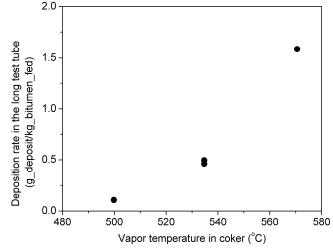is fixed. As $T_R$ is raised, with the test section wall temperature held constant, the amount of deposits increases as shown in Figure 3.



Figure 3 Effect of coker temperature $T_R$ on deposit yield at fixed test section temperature, $T_D = 535°C$.

For fixed $T_R$, the deposition yield remained constant at $T_D>T_R$, even up to $T_D$ values of over 600°C (Figure 4). This suggested that deposition was not caused by more severe coking reactions. When the vapours from the coker were cooled below $T_R$, deposition increased dramatically, presumably due to physical condensation. In Figure 5, the deposition rate is seen to increase with the temperature driving force for physical condensation, $(T_R–T_D)$. Other experiments (Zhang and Watkinson, 2005) showed that as the concentration of heavy hydrocarbon vapours was reduced by adding extra secondary steam, deposition decreased. As the velocity was raised from 2.2 to 16.4 m/s by changing the test section tube diameter, there was no effect on deposition rate. Deposits were found to vary in carbon content, depending on temperature. The H/C atomic ratio of fresh deposits decreased from 0.6 at vapour temperature of 440°C, to 0.35 at 610°C. Aging of deposits was also investigated.
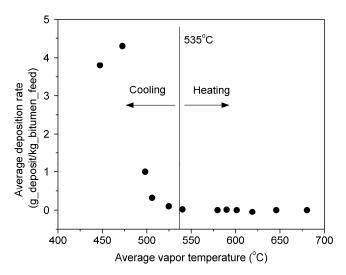


Figure 4 Effect on deposition rate of test-section vapour temperature, $T_D$, at $T_R = 535°C$.

**Comparison of Lab and Industrial Conditions**

Table 1 compares lab and plant clean-tube conditions. In order to match vapour compositions in lab and plant, the vapour phase residence times in the coker were matched. However, lab deposition experiments were carried out under laminar flow conditions (Re=530–1430), whereas in the plant Re~1.5E06, although superficial velocities were not that much different at 10 m/s in lab, and 40 m/s in the plant. As seen in Table 1, there was also a difference in clean wall shear stress.
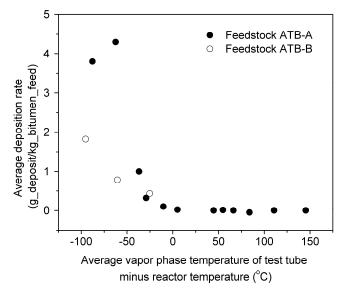


Figure 5 Deposition rate versus temperature difference $(T_D - T_R)$ for varying $T_R$ (500–570ºC) and $T_D$ (450–680°C).

Phase equilibrium calculations using HYSYS suggested that in both lab and plant, a small amount of liquid phase would be present in the vapours. Estimated droplet concentrations were an order of magnitude higher in the plant than in the lab (Table 1). Some droplet deposition calculations were therefore undertaken.

Table 1 Comparison of Conditions in Lab and Plant.

| | d, mm | L/d, - | V, m/s | Re, - | $\tau_w$, Pa | Pe (d/L), - | $C_b$, g/m$^3$ | $v_V \cdot 10^5$, m$^2$/s | $\rho_D$, kg/m$^3$ |
|---|---|---|---|---|---|---|---|---|---|
| Lab | 5.8 – 15.7 | 57 – 155 | 2 – 17 | 500 – 1400 | 0.25 | >1E+07 | 3 | 7 | 1270 |
| Plant | 670 | 7.8 | 40 | 1.5 E06 | 15.1 | >1E+10 | 50 | 2 | 760 |

$(T_0 = 540°C, q = −4.9$ kW/m$^2)$

**Droplet deposition calculations for the cyclone exit line**

The lab unit had been modeled in two-dimensions from first principles considering physical condensation on the wall of a single pseudo-component in a mixture of vapour and gas (Zhang and Watkinson, 2005). With some assumptions, the trend of average deposition rate versus gas stream temperature could be predicted, and using molecular mass of the heavy component as a fitting parameter, the lab data could be fitted. However, it was unclear whether bulk condensation leading to droplet formation was also a factor in the lab unit, and if wall condensation was significant in the industrial unit. Therefore, droplet deposition rates were estimated (Fan, 2006).

Assumptions for the one-dimensional models included: constant inlet molar flow and composition with time, plug flow of vapour/gas mixture with suspended droplets of a specified size in a smooth circular tube; fully developed flow; Inlet temperature fixed at $T_0$; constant and uniform wall heat flux; constant properties with length. For the lab unit, laminar flow was assumed, with droplet transport by diffusion. In the plant unit, flow was turbulent, and droplet transport occurred by diffusion, inertia or impaction. Perfect sticking was assumed in both situations. Given the above assumptions, the energy balance gives the axial fluid temperature profile,

$$\frac{dT}{dz} = \frac{q\pi d}{F_{droplet,0}(1-x)C_{p,droplet} + F_{vapour}C_{p,vapour}} \quad (1)$$

The droplet component mass balance equation is:

$$\frac{dx}{dz} = \frac{R_d \pi d}{F_{droplet,0}} \quad (2)$$

Here $F$ represents molar flow rate (mol/s), $x$ is the fraction of droplets converted into deposits, and $R_d$ the droplet deposition flux (mol/m$^2$s). The deposit thickness $\delta_c$ is calculated from the deposition flux as described later, which is in general form,

$$\delta_c = \delta_c(z,t) \quad (3)$$

The model is pseudo-steady-state with respect to time. The solution of equations (1) and (2) is assumed constant over a time step, and the effects of the deposit accumulation through equation (3) are updated explicitly at the end of each time step. This pseudo-steady-state assumption would be indeed valid as long as the deposit formation rate does not change appreciably over a sufficiently small time step. Changes to velocity and pressure drop with blockage are given by equations (4) and (5).

$$\frac{V_{fouled}}{V_{clean}} = \frac{D^2}{(D - 2\delta_c)^2} \quad (4)$$

$$\frac{\Delta P_{fouled}}{\Delta P_{clean}} = \frac{D^5}{(D - 2\delta_c)^5} \quad (5)$$

The pressure drop increase at constant throughput could limit the run length in practical operation, leading operators to reduce throughput when a given pressure drop is reached. For the sake of simplicity, the present study is limited to a constant inlet mass flowrate.

The transport of liquid droplets from the mainstream to the deposition surface can be expressed as:

$$R_d = k_t(C_b - C_s) = k_d C_b \quad (6)$$

in which $C_b$ is the bulk concentration of liquid droplets, and $C_s$ is concentration of droplets in suspension adjacent to deposition surface. If it is assumed that all droplets that arrive at the tube surface adhere to it, $C_s = 0$ and the transport coefficient $k_t$ becomes identical to the deposition coefficient $k_d$. The mass transfer coefficient calculation for laminar flow is given as equation (7). For turbulent flow,

equations for diffusion, inertial and impaction regimes cited by Epstein (1997) were used, with hydrodynamic and thermal entrance region effects ignored.

$$Sh = \frac{k_m d}{D_e} = 1.62(Pe\frac{d}{L})^{1/3} \qquad (7)$$

For the laminar flow case, for droplets of 1 and 10 microns, calculated droplet deposition rates were in the range 1–4E-06 g/m²-s, a factor of roughly 300 to 3500 below experimental or wall condensation model values. Thus droplet transport with perfect sticking was ruled out as a significant mechanism in the lab unit.

For turbulent flow, with larger sized droplets the deposition mechanism shifts from diffusion to impaction, which accelerates the droplet deposition rate dramatically and causes much more deposit in the tube entrance region. Figure 6 shows the increase in pressure drop, deposit layer thickness, transport coefficient and velocity as deposition proceeds for three droplet sizes. Very small droplets ($d_p$ = 0.1 μm) where diffusional mass transfer has a role, results in extensive blockage within 300-days. Somewhat larger droplets ($d_p$ = 1 μm) extend the operating time to about 1000 days, due to the decrease in droplet diffusivity. At droplet diameters of 2 μm, inertial effects begin to be important, and blockage effects appear significant after some 80-days. It must be stressed that these illustrative calculations do not include any droplet suppression of adhesion or removal
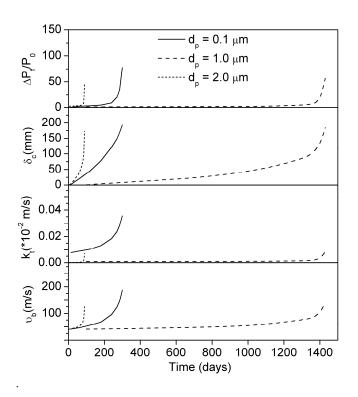


Figure 6  Increases of pressure drop, deposit thickness, transport coefficient and bulk velocity versus time on stream

effects, which could well be significant at the wall shear stresses involved. The high wall shear stress in the industrial unit would tend to cause removal of any condensed liquid. Clearly, information on droplet size distribution, effects of wall shear stresses on removal or suppression of deposition, and droplet concentration is critical to predicting pressure drop versus time in such units.

## SCRUBBER GRID FOULING

Conditions in the scrubber grid are very different than in the cyclone exit line, however the source of fouling may be similar. Heavy hydrocarbon species of boiling points (>524ºC) which arise in the coker can pass through the cyclone exit line into the scrubber. If this material is not removed in the shed section of the scrubber, it will impact the bottom of the grid. Figure 7 shows elements of the grid, which is a structured packing of high (ca. 97%) voidage. The grid operates at temperatures of around 390ºC. The packing geometry is complex, and has been designed for fouling services (Pham, 1997). The grid is irrigated, however there are uncertainties in the uniformity of liquid flow in large diameter units. A clean and a severely fouled segment of the grid is shown as Figure 8.
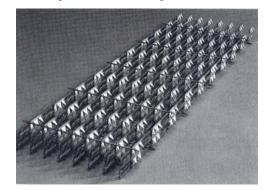


Figure 7 Packing elements in grid (approximate dimensions 7 cm × 40 cm × 150 cm).



Figure 8 Segment of grid blade under clean and severely fouled conditions.

As the blades are bent out from the vertical, flow through the packing is obviously very complex, and has upstream and downstream surfaces. For the laboratory studies, flow normal to a circular disk, which has both upstream and downstream surfaces, was chosen. Experiments were limited to non-irrigated conditions.

## Experimental apparatus and procedures

To investigate the effect of process variables on deposition, a bench-scale unit was constructed (Figure 9). The spray chamber, an externally heated 7.5-cm-diameter ×

1.0-m-length pipe, contained the atomization nozzle, and the test disk. The 5-cm-diameter disk on which the deposits form, was located 75 cm above the nozzle, and was attached to a load-cell by means of a rod. At this distance from the atomizer, the gas velocity profile is established and is relatively uniform, based on CFD simulation (Lakghomi, 2009). Six drain holes were drilled in the disk around the center hole which connects with the rod, such that droplets from the rod flowed down through the holes and did not significantly affect the deposition rate on the disk surface. The disks were made of 1.2-mm thick type 304 stainless steel with a 2B finish. Oil which flowed down the spray chamber wall was collected such that knowing the oil feed rate, and the average wash-down rate, the flow of oil droplets carried past the disk could be calculated by difference. The heavy oil (MEBR) which contained the carbonaceous deposit-forming components was mixed in different concentrations with lighter diluent oil (VE) to lower the viscosity for ease of pumping and atomization (Table 2).
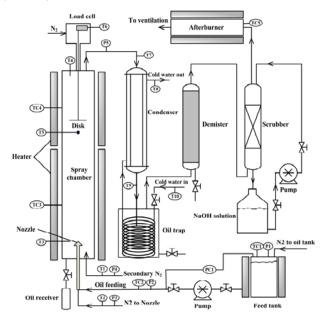


Figure 9  Schematic representation of the Hot Unit setup (Song et al., 2011).

The oil mixture at 100°C was atomized with pre-heated nitrogen, and secondary nitrogen was added to establish the desired gas velocity. A two-fluid atomizer was used. Volume mean droplet diameters are estimated to be in the range 2.3−5.3 microns, based on a correction to room-temperature measurements made using tri-ethylene glycol. A 100-gram load cell was used to monitor the total mass change of the disk, rod and the deposits on them with time. At the end of a run, the accumulated mass on the disk was measured by weighing on an analytical balance to provide a check with the load-cell data. The deposit amount on the rod was measured. The mass on the upstream and downstream side of the disk was separately determined in selected experiments.

Table 2 Selected properties of oils.

| Oil | MEBR | VE |
|---|---|---|
| Density (g/mL) | 1.033 | 0.877 |
| H/C (atomic) | 1.48 | 1.87 |
| IBP (°C) | 283 | 218 |
| % Distilled at 343°C | 3.2 | 71 |
| % Distilled at 524°C | 30.6 | 100 |
| Metals (wt %) | 1.25 | ND |

As temperature is increased, deposition rate decreases as the concentration of heavy components present as liquid decreases. Load cell and analytical balance show good agreement (Figure 10) for total deposition. On the disk itself, deposition is clearly less with 5% MEBR in the oil blend, than at 10% MEBR. Deposition on the rod is nearly independent of temperature and MEBR concentration. As the percentage of MEBR in the blend is raised at fixed temperature, deposition rate increases in linear manner (Song et al., 2011).
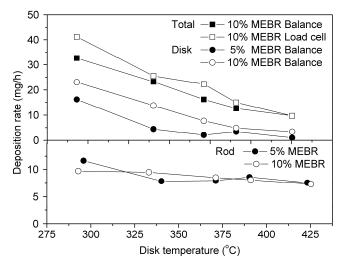


Figure 10 Effect of aerosol temperature on deposition rate of the disk and the rod for two MEBR concentrations.

Table 3 shows that as temperature increases, the composition of the deposits changes from essentially that of the MEBR, to a coke-like material with H/C ~ 0.8, and ash content over 5%. Industry samples show lower H/C ratio due to ageing phenomena.

Table 3 Comparison of deposit compositions at different disk temperatures.

| Sample | MEBR | T = 293°C | T = 390°C | Industry |
|---|---|---|---|---|
| H/C | 1.48 | 1.42 | 0.77 | 0.4 |
| % ash | 1.68 | 3.0 | 5.4 | 6.5 |

Velocity effects over the range 0.2 to 0.9 m/s  were weak, and showed some scatter (Figure 11). At low velocities, deposition occurs mainly on the downstream surface. As velocities are raised, droplet capture on the upstream surface becomes increasingly important, as will be discussed further below.

Droplet concentrations which could not be readily measured under Hot Unit conditions were estimated using HYSYS. Calculations were based on a property package consisting of the Peng-Robinson equation of state, and a set of hypothetical petroleum components, user specified bulk properties and distillation curves of VE and MEBR. The mass fractions of liquid and vapour, and other calculated properties were used to estimate droplet concentrations and properties for CFD calculations. Figure 12 shows deposition rates measured versus calculated droplet concentrations.
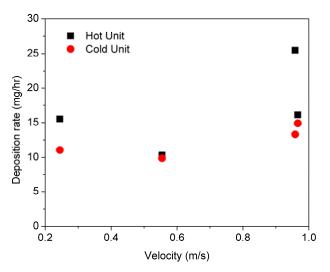


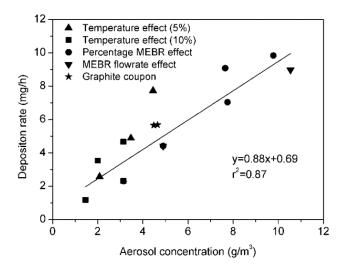Figure 11 Effect of velocity in Hot Unit and with the predictions from the Cold Unit deposition coefficients.



Figure 12 Effect of calculated droplet concentration on deposition rate at fixed velocity.

## Comparison of Lab and Industrial Conditions

Table 4 compares the lab conditions of the flow normal to a circular disk, and plant conditions with irrigated flow over a complex packing. For the packing, an equivalent diameter of 8.6 cm was calculated based on pressure drop and a particle bed model. Three levels of modeling were used to interpret the lab data.

Table 4 Summary of lab (circular disk) and plant (structured packing) conditions.

| Unit | d, mm | Irrig'n | T, °C | V, m/s | $C_b$, g/m³ | $d_{eq}$, mm | $Re_{eq}$, - | $\tau_W$, mPa |
|------|-------|---------|-------|--------|-------------|--------------|--------------|----------------|
| Plant | 9000 | Yes | 390 | 1 | 750 | 86 | 520 | 15 |
| Lab | 75 | No | 290–420 | 0.2–0.9 | 2–10 | 50 | 210–870 | 1–8 |

***Physical modeling of lab Hot Unit:*** A room temperature system (Cold Unit) using try-ethylene glycol and air (Petkovic, 2009) was used as a physical model of the lab Hot Unit. Here, concentrations of droplets, drop sizes and contact angles could be measured, and a wider range of superficial gas velocities covered. Deposition rates were determined from the mass of deposits at the end of each experiment, since online measurements via load cell confirmed constant deposition rates with time. Size distribution of droplets in the Cold Unit was determined via a shadowgraphy method. The distributions were log-normal, with volume median diameter between 3.9 and 7.5 microns. Concentration of droplets was determined via two methods: (a) using shadowgraphy and (b) from the flow of liquid to the aerosol that was calculated by subtracting the washdown flow rate from the liquid flow rate to the nozzle. The concentration varied from 6 to 12 g/m³. Contact angles of tri-ethylene glycol droplets on the disk surface, which can make a difference between sticking or rebounding, were measured using the shadowgraphy setup. For three different surfaces, namely glass, stainless steel and Teflon, contact angles were 20°, 51° and 94° respectively. No significant effect of contact angle on deposition coefficients was observed.

The results showed that deposition coefficients (and deposition rates) on the upstream side increased significantly with the increase in drop diameter due to predominant inertial impaction of rare large droplets. Deposits were concentrated more toward the edge of the disk. Deposition coefficients for the downstream side increased less sharply with the increase in droplet diameter. The downstream side collected intermediate size droplets that were uniformly distributed on the surface.

By increasing the superficial velocity, deposition coefficients on the upstream side increased according to the theory of inertial impaction, while on the downstream side, deposition coefficients showed minimum with velocity at about 0.6 m/s. The upstream surface collected up to 10 times more deposits at high end of the velocity range (1–1.5 m/s).

By measuring size distribution of droplets on the disk and in the aerosol, it was possible to obtain deposition coefficients for individual droplet sizes. When the data are expressed in terms of capture efficiencies ($E = k_d / V$) and plotted vs. Stokes number ($St = \rho_p d_p^2 V / 18\mu D_c$) at different velocities, Figure 13 is obtained.

The change in Stokes number due to changes from room temperature to Hot Unit conditions (different gas viscosity and droplet density) can be calculated by

$$St_{HU} = St_{CU} \ \frac{\rho_o \ \mu_v^{-1}}{\rho_{EG} \ \mu_A^{-1}} \ . \qquad (8)$$

Since capture efficiencies can be approximated with a linear dependence on Stokes number in the region of small Stokes numbers ( $E = k \, St$ , Figure 13), a prediction for the capture efficiency in the Hot Unit can be obtained:
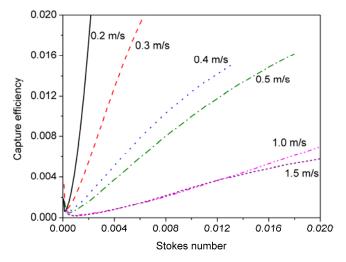


Figure 13 Capture efficiencies calculated from experimental results for the downstream side vs. Stokes number, in the range of droplet sizes (1–20 microns) and velocities (0–1.5 m/s).

$$E_{HU} = E_{CU} \ \frac{\rho_o \ \mu_v^{-1}}{\rho_{EG} \ \mu_A^{-1}} \ . \qquad (9)$$

When deposition rates for 10% MEBR in the Hot Unit were calculated from the room temperature data and equations (8, 9), relatively good agreement was obtained (Figure 11, Figure 14).
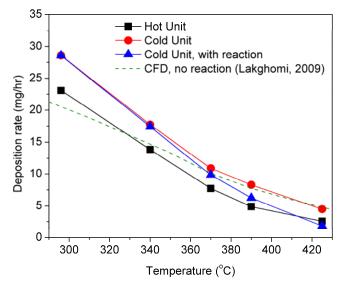


Figure 14. Comparison between Hot Unit deposition rates for 10% MEBR, with the predictions from the Cold Unit deposition coefficients, and CFD predictions

***CFD model of the lab Hot Unit:*** Lakghomi calculated the hydrodynamics and droplet transport to the upstream and downstream surfaces of the lab Hot Unit using FLUENT, and utilized HYSYS for mixture phase equilibrium (Lakghomi, 2009, Lakghomi *et al*., 2011). Droplet rebounding excess energy calculations supported the case for perfect sticking for the system used. Figure 14 includes a curve showing predictions of the CFD model for the disk as a function of temperature. For $St$<0.008, capture efficiencies for the downstream surface exceeded that for the upstream surface. Calculated ratios of downstream to upstream deposition rates were found to be 25 to 12 for droplets of 1 to 10 microns, at a velocity of 0.2 m/s, and decreased to values close to unity at 0.9 m/s. These values reflected ratios observed experimentally of 9 to 19 at V = 0.24 m/s.

***Scrubber model using HYSYS:*** Subudhi used HYSYS to calculate physical and thermodynamic properties in the system and to model the contact and separation processes (Subudhi, 2009). The Bravo-Rocha-Fair model was used to calculate pressure drop for the grid packing in counter-current flow. Transport and attachment models for the droplets to both wetted and non-wetted surfaces were used to calculate the total mass of droplets which stick to the surface per unit time. The mass of carbonaceous solid formed per unit time was calculated using available coking kinetics. As the coke layer grows, voidage in the packing decreases, and pressure drop increases. The overlapping of deposits from various parts of the packing surface was included in the calculation. Calculations indicated the role of wetting, droplet size, wash oil flows and temperature on the deposit build-up with time.

## CONCLUSIONS

Two experimental studies of equipment fouling from heavy hydrocarbon systems illustrate problems in applying lab data to plant conditions:

**1.** For heavy hydrocarbon fouling from the vapour-phase, lab results taken in the laminar flow indicated that physical condensation onto the wall was the root cause of deposition. For the plant, bulk condensation appeared to be the primary cause of fouling. Although velocities in the lab were close to those in the plant, the high Reynolds no. and wall shear stress of the latter could not be matched. Simple transport models show the importance of droplet size for plant conditions, but did not account for adhesion processes.

**2.** Deposition of fine droplets on a circular disk at low Stokes number showed highest rates on the downstream side of the disk, in agreement with CFD modeling. Results from a room temperature physical model system gave support to the Hot Unit studies. Results could be applied to the non-wetted portion of a scrubber grid, as Reynolds numbers and wall shear stresses can be roughly matched.

**3.** For both cases, reliable physical property and phase behavior calculations are essential. However, application of existing codes to heavy hydrocarbons raises uncertainties.

## NOMENCLATURE

| | |
|---|---|
| A | area ($m^2$) |
| $C_b$, $C_s$ | bulk, surface droplet concentration ($g/m^3$) |
| $C_p$ | molar heat capacity (kJ/mol°C) |
| d, $d_e$, $d_p$ | tube, equivalent, droplet diameter (m) |
| $D_c$ | disk diameter (m) |
| $D_e$ | diffusivity ($m^2/s$) |
| E | collection efficiency (dimensionless) |
| F | molar flowrate (mol/s) |
| k | constant (dimensionless) |
| $k_d$ | deposition coefficient (m/s) |
| $k_m$ | mass transfer coefficient (m/s) |
| $k_t$ | transport coefficient (m/s) |
| L | length to tube (m) |
| P | pressure (Pa) |
| $R_d$ | droplet deposition flux ($mol/m^2$-s) |
| t | time (s) |
| T | temperature (K) |
| V | superficial velocity (m/s) |
| x | mass fraction droplets deposited (dimensionless) |
| Z | distance along tube (m) |
| Pe | Peclet number (dimensionless) |
| Re | Reynolds number (dimensionless) |
| Sh | Sherwood number (dimensionless) |
| St | Stokes number (dimensionless) |
| δ | deposit thickness (m) |
| ν | kinematic viscosity ($m^2/s$) |
| ρ | density ($kg/m^3$) |
| μ | dynamic viscosity (Pa·s) |
| τ | wall shear stress (Pa) |

### Subcripts

| | |
|---|---|
| 0 | initial |
| A | air |
| CU | Cold Unit |
| D | deposition test section |
| EG | tri-ethylene glycol |
| HU | Hot Unit |
| o | oil |
| R | coker reactor |
| v | vapour |
| W | wall |

## REFERENCES

Epstein, N., 1997, Elements of particle deposition onto non-porous solid surfaces parallel to suspension flows, *Experimental Thermal and Fluid Science,* Vol. 14, pp323-334.

Hammond, D. G., 1998, Tutorial: Fluid Coking/Flexicoking Fundamentals, *International Conference on Refinery processes*, Topical Conference Pre-prints, AIChE, March 9-11, New Orleans, La, USA pp170-181.

Lakghomi, B., Taghipour, F., Posarac, D., and Watkinson, A.P., 2011, CFD simulation of aerosol flow and hydrocarbon fouling on a circular disk, *Chemical Engineering Journal, Vol. 172,pp507-516.*

Lakghomi, B., 2009, *CFD simulation of aerosol flow and hydrocarbon fouling on a circular disk*, M.A.Sc. Thesis, The University of British Columbia, Canada.

Mallory, D.G., Mehta, S.A., Moore, R.G., Richardson, S., 2000, The Role of the Vapour Phase in Fluid Coker Cyclone Fouling:Part 1. Coke Yields, *Canadian Journal of Chemical Engineering,* Vol. 78, pp330-336.

Petkovic, B., 2010, *Deposition of Droplets onto Solid Objects in Aerosol Flow,* M.A.Sc. Thesis, The University of British Columbia, Canada.

Pham, L.V., 1997, High-Performance Anti-Fouling Tray Technology and Its Application in the Chemical Industry, Pre-print, *AICHE Spring National Meeting*, Houston TX, USA, 12 March 1997.

Song, J., Watkinson, A.P., Taghipour, F., Posarac, D., and Petkovic, B., (2011) Deposition of Heavy Oil Droplets onto a Circular Disk at Elevated Temperatures, Submitted to *Industrial and Engineering Chemistry Research,* Nov. 2011.

Subudhi, N., 2006, *Simulation of pressure drop and coke deposition in the grid of a scrubber*, M.A.Sc. Thesis, The University of British Columbia, Canada.

Wiehe, I. A., 2008, *Process Chemistry of Petroleum Macromolecules,* CRC Press, USA.

Zhang W., and Watkinson, A. P., 2005, Carbonaceous Material Deposition from Heavy Hydrocarbon Vapors 1. Experimental Investigation, and 2. Mathematical Modeling, *Ind. Eng. Chem. Res.* Vol. 44, pp4084-4091, 4092-4098.